Magneto-Inertial Dead-Reckoning Navigation with Walk Dynamic Model in Indoor Environment

Raphaël Neymann, Alexis Berthou, Jean-François Jourdas, Hugo Lhachemi, Christophe Prieur, Antoine Girard

Magneto-Inertial Dead-Reckoning Navigation with Walk Dynamic Model in Indoor Environment

Raphaël Neymann[1,2], Alexis Berthou[2], Jean-François Jourdas[2],
Hugo Lhachemi[1], Christophe Prieur[3], and Antoine Girard[1]

***Abstract*—We tackle the problem of pedestrian indoor navigation with Magneto-Inertial Dead Reckoning technology (MIDR) with the integration of the data provided by a Magneto-Inertial Measurement Unit (MIMU). This method is well-known in the literature and very efficient if the spatial distribution of the magnetic field is nonuniform and the gradient of sufficiently high magnitude. However, the quality of the magnetic information decreases as the pedestrian moves toward a weak magnetic zone. We propose, characterize and test a new correction technique of the MDIR velocity based on the detection of walking steps and dynamical modeling of the walk itself.**

I. INTRODUCTION

Dead-Reckoning navigation (DR) consists in the estimation of the dynamics of a system moving in an unknown environment. It requires the measurements of inertial data : acceleration and angular velocity. Dead-Reckoning navigation are generally updated with an outer correction term, which can be coming from an optical information, a direct velocity measurement – *e.g.* GNSS – or the measurement of a characteristic physical field. Optical information and GNSS measurements are not reliable indoor where GNSS signals can be blocked, and good lightning conditions are not guaranteed. However, indoor, the magnetic field is high and the instantaneous measurement of the magnetic field and its time and space variations provide important information about the motion of the body. The principle of Magneto-Inertial Dead-Reckoning (MIDR) is to combine inertial data with a spatial mapping of the magnetic environment. During the last past decade, MIDR has been widely improved and explained in the literature for any indoor navigation [2], [5], [14] or odometry [12], in particular the modelling of Maxwell's fields equations in the dynamic equations. This method is especially interesting for the estimation of the heading in an indoor environment [3] and has the property to naturally bound the divergence due to the instability of inertial sensors linearly in time.

However, if the magnetic field is spatially uniform, a loss of observability occurs. Weak magnetic gradient phases can no longer be handled by the magnetic corrections. Moreover, miscalibration effects can be amplified during a low-gradient phase [4]. Therefore, another correction term shall be added to the MIDR model. Artificial Neural Networks (ANN) have been used as a complement of magnetic data [18], *e.g.* with the use of BiLSTM in the determination of the different phases of walk with learning; as well as infrastructured ways such as Ultra-Wide Band (UWB) or WLAN. However, a more common approach is to add a *Zero Velocity Update* (Zupt) term to the dynamic system [11], [17]. In this situation, if a motionless phase is detected in the inertial data – accelerometric and gyrometric – through a threshold fast test – *e.g.* a comparison with the noise rate of these sensors –, the velocity is forced to be zeros during this period.

For pedestrian indoor navigation, it is then interesting to consider an additional velocity information through step-detection. However, Zupt is often too restrictive as it requires to put the navigation device at a specific location on the foot and is very sensible to shocks. As a result, a more generic approach was developed and patented in [15], [16]: the phases of a typical walk pattern are detected and the velocity is computed from a walk model eliminating the part due to the leg or body relative motion. Contrarily to the Zupt approach, the walk pattern does not force the velocity to be zeros but is modeled by a formula that involves the angular velocity and a geometric parameter determined by the position of the accelerometer relatively to the ankle of the pedestrian operator. Therefore, the Zupt becomes a particular situation of this walk model when the angular velocity tends to vanish.

This paper proposes a fusion between classic MIDR and the velocity issued from step-detection and walk specific motions. First, we recall important notions of inertial and magnetic navigation (Section II), which are useful to the design of an Extended Kalman Filter and its theoretical analysis (EKF) (Section III). We derive the conditions of observability and good performance of the MIDR technology, which highlights the interest of an additional velocity measurement to cover some weak observability conditions occurring in practice. We then recall the principles of a velocity estimation technique based on step-detection and walk specific motion. Finally, we present a novel fusion scheme between MIDR and the velocity derived from the walk motion (Section IV) and present improved navigation results obtained on a typical indoor scenario (Section V).

II. PRELIMINARIES

A. Frames and rotations

A vector $\mathbf{u} \in \mathbb{R}^3$ expressed in the navigation frame $\mathscr{R}^{\mathrm{n}}$ are denoted by an upperscript n, *i.e.* $\mathbf{u}^{\mathrm{n}}$. Conversely, this latter is expressed in the body frame $\mathscr{R}^{\mathrm{b}}$ are denoted by an upperscript

[1] Université Paris-Saclay, CNRS, CentraleSupélec, Laboratoire des Signaux et Systèmes, 91190 Gif-sur-Yvette, France
[2] SYSNAV, 27200 Vernon, France
[3] Université Grenoble Alpes, CNRS, Grenoble-INP, GIPSA- lab, 38000 Grenoble, France. The work of this author has been partially supported by MIAI@Grenoble Alpes (ANR-19-P3IA-0003).

b, *i.e.* $\mathbf{u}^{\mathrm{b}}$. The rotation rate, provided by the gyrometer, from the body frame $\mathscr{R}^{\mathrm{b}}$ to the navigation frame $\mathscr{R}^{\mathrm{n}}$ is denoted by

$$\mathbf{\Omega}^{\mathrm{b/n}} = \begin{pmatrix} 0 & -\omega_z^{\mathrm{b/n}} & \omega_y^{\mathrm{b/n}} \\ -\omega_z^{\mathrm{b/n}} & 0 & -\omega_x^{\mathrm{b/n}} \\ -\omega_y^{\mathrm{b/n}} & \omega_x^{\mathrm{b/n}} & 0 \end{pmatrix} \in \mathfrak{so}(3), \tag{1}$$

element of the tangent space of the rotation group $\mathrm{SO}(3)$. By convention, the attitude $\mathbf{R} \in \mathrm{SO}(3)$ maps a vector in the body frame $\mathbf{u}^{\mathrm{b}}$ to its equivalent in the navigation frame $\mathbf{u}^{\mathrm{n}} = \mathbf{R}\mathbf{u}^{\mathrm{b}}$.

B. Magneto-Inertial Measurement Unit (MIMU)

The MIDR technology requires the measurement of the local magnetic field $\mathbf{B}^{\mathrm{b}}$ and its space gradient

$$\mathbf{B}^{\mathrm{b}} = \begin{pmatrix} B_x^{\mathrm{b}} \\ B_y^{\mathrm{b}} \\ B_z^{\mathrm{b}} \end{pmatrix}, \quad \nabla\mathbf{B}^{\mathrm{b}} = \begin{pmatrix} \partial_x B_x^{\mathrm{b}} & \partial_y B_x^{\mathrm{b}} & \partial_z B_x^{\mathrm{b}} \\ \partial_x B_y^{\mathrm{b}} & \partial_y B_y^{\mathrm{b}} & \partial_z B_y^{\mathrm{b}} \\ \partial_x B_z^{\mathrm{b}} & \partial_y B_z^{\mathrm{b}} & \partial_z B_z^{\mathrm{b}} \end{pmatrix} \tag{2}$$

in the body frame [5]. Magnetic raw data are sensed through a space array of n magnetometers, disposed with a given and known geometry relatively to the position of the accelerometer on the sensors board [2], [4], [7], providing vector measurements $\mathbf{M}_1, \mathbf{M}_2, \ldots, \mathbf{M}_n \in \mathbb{R}^3$. The sensors composing the array are also supposed to be calibrated with a linear model correcting scale factors and misalignments – expressed in a nonsingular matrix $\mathbf{A}_k \in \mathrm{GL}(3)$ – and biases – wrapped in vectors $\mathbf{b}_k \in \mathbb{R}^3$ –

$$\mathbf{B}_k^{\mathrm{b}} = \mathbf{A}_k \mathbf{M}_k + \mathbf{b}_k, \tag{3}$$

where $\mathbf{B}_k^{\mathrm{b}}$ is the calibrated data of sensor k [4], [9]. This model describes the contributions of soft and hard iron for each individual 3D magnetometer. The fusion of all calibrated data is thereafter achieved by a linear combination of these data to estimate the values of the components of $\mathbf{B}^{\mathrm{b}}$ and $\nabla\mathbf{B}^{\mathrm{b}}$ [5], ending the complete process of calibration. In the following, we denote by *miscalibration* any error in the identification of the calibration parameters – *e.g.* in biases or scale factors.

The magnetic data are completed with inertial measurements sensed by an Inertial Measurement Unit (IMU). An accelerometer provides the measurement of the proper acceleration $\boldsymbol{\gamma}^{\mathrm{b}} \in \mathbb{R}^3$. The constant gravity acceleration is denoted by $\mathbf{g}^{\mathrm{n}} \in \mathbb{R}^3$ and is expressed in the navigation frame. Moreover, a gyrometer – which provides the angular velocity $\mathbf{\Omega}^{\mathrm{b/n}}$ – is supposed to be located at a position $\boldsymbol{\ell}^{\mathrm{b}}$ relatively to the accelerometer. The IMU data are assumed to be also well calibrated with a specific model.

The MIMU is embedded in a hardware device – produced and developed by the company Sysnav – which is attached to the ankle of a pedestrian operator by straps, as shown on Fig. 1. The position near the ankle is necessary for the step detection and the use of a walk dynamic model.

C. Magnetic field structure

In this paper, we assume a static magnetic field $\mathbf{B}$, *i.e.* which is time-independent: $\partial\mathbf{B}/\partial t = \mathbf{0}$. In indoor conditions, the MIDR device moves within a space region in which it is assumed that there is no electric current $\mathbf{J}$ nor electric field $\mathbf{E}$. This hypothesis yields important properties due to static Maxwell's equations, which are equivalent to the ones expressed in vacuum[1]:

$$\nabla \cdot \mathbf{B} = 0, \quad \nabla \times \mathbf{B} = \mathbf{0}. \tag{4}$$

Proposition 1: The magnetic gradient $\nabla\mathbf{B}$ can be orthogonally decomposed in eigenvectors and real eigenvalues [5]

$$\nabla\mathbf{B} = \mathbf{U} \begin{pmatrix} \lambda & 0 & 0 \\ 0 & \mu & 0 \\ 0 & 0 & -\lambda-\mu \end{pmatrix} \mathbf{U}^{\top}, \quad \lambda, \mu \in \mathbb{R}, \quad \mathbf{U} \in \mathrm{SO}(3). \tag{5}$$

Fig. 1: Sysnav's MIMU attached to the ankle of a pedestrian.

III. THEORY OF MAGNETO-INERTIAL DEAD RECKONING

A. Kinematics of the magnetic field

The kinematic equation of the MIDR is based on the space and time variations of the magnetic field in an inhomogeneous field – *i.e.* in the presence of a gradient [3], [14]:

$$\dot{\mathbf{B}}^{\mathrm{b}} = -\left(\mathbf{\Omega}^{\mathrm{b/n}} - \mathbf{\Omega}_{\mathrm{b}}^{\mathrm{b/n}}\right)\mathbf{B}^{\mathrm{b}} + \nabla\mathbf{B}^{\mathrm{b}}\mathbf{v}^{\mathrm{b}}. \tag{6}$$

Definition 1: **Magnetic velocity.** The magnetic velocity consists in the velocity isolated from Eq. (6)

$$\mathbf{v}_{\mathrm{mag}}^{\mathrm{b}} = \left(\nabla\mathbf{B}^{\mathrm{b}}\right)^{-1}\left[\mathbf{\Omega}^{\mathrm{b/n}}\mathbf{B}^{\mathrm{b}} + \dot{\mathbf{B}}^{\mathrm{b}}\right], \tag{7}$$

provided the nonsingularity of the magnetic gradient $\nabla\mathbf{B}^{\mathrm{b}}$.

[1]Maxwell's equations in vacuum are invariant by translations and rotations, so these results either hold in the body or the navigation frame.

It follows from the previous Def. (1) that $\mathbf{v}_{\text{mag}}^{\text{b}}$ is conditioned by the gradient $\nabla\mathbf{B}^{\text{b}}$, and especially its conditioning number $\kappa = \max_i|\lambda_i|/\min_i|\lambda_i|$ which quantifies the observability of the motion. The structure of the magnetic gradient developed in II-C implies that the eingenvectors and values are interdependent. Different configurations can then happen up to a multiplication by κ, the situation where the eigenvalues are $(1|1|-2)$ is favorable due to the observability of each direction but only if the lowest eingenvalue is not to small; the situation $(1|-1|0)$ is contrarily not desirable because the magnetic field is constant toward the weakest direction, which is consequently not observable.[2]

B. Extended Kalman Filter design

The equation of motion Eq. (6) can be plugged into an Extended Kalman Filter (EKF) [2], [5], [8], [13], [14], combined with the estimation of the attitude $\mathbf{R} \in \text{SO}(3)$ and the inertial biases $\hat{\boldsymbol{\Omega}}_{\text{b}}^{\text{b/n}}$ and $\hat{\boldsymbol{\gamma}}_{\text{b}}^{\text{b}}$:

$$\begin{cases} \dot{\hat{\mathbf{R}}} & = \hat{\mathbf{R}}\left(\boldsymbol{\Omega}^{\text{b/n}} - \hat{\boldsymbol{\Omega}}_{\text{b}}^{\text{b/n}}\right) \\ \dot{\hat{\mathbf{v}}}^{\text{b}} & = -\left(\boldsymbol{\Omega}^{\text{b/n}} - \hat{\boldsymbol{\Omega}}_{\text{b}}^{\text{b/n}}\right)\hat{\mathbf{v}}^{\text{b}} + \boldsymbol{\gamma}^{\text{b}} - \hat{\boldsymbol{\gamma}}_{\text{b}}^{\text{b}} + \hat{\mathbf{R}}^{\top}\mathbf{g}^{\text{n}} \\ \dot{\hat{\mathbf{B}}}^{\text{b}} & = -\left(\boldsymbol{\Omega}^{\text{b/n}} - \hat{\boldsymbol{\Omega}}_{\text{b}}^{\text{b/n}}\right)\hat{\mathbf{B}}^{\text{b}} + \nabla\mathbf{B}^{\text{b}}\hat{\mathbf{v}}^{\text{b}} \\ \dot{\hat{\boldsymbol{\Omega}}}_{\text{b}}^{\text{b/n}} & = \mathbf{0} \\ \dot{\hat{\boldsymbol{\gamma}}}_{\text{b}}^{\text{b}} & = \mathbf{0}. \end{cases} \tag{8}$$

The value $\nabla\mathbf{B}^{\text{b}}$ of the magnetic gradient comes from the magnetic measurement unit. This filter is corrected through the outer observation of the magnetic field $\mathbf{z} = \mathbf{B}^{\text{b}}$ measured from the magnetometer array. This observation is compared with the measurement of the magnetic field $\mathbf{y} = \hat{\mathbf{B}}^{\text{b}}$ through the projector $\mathbf{h}\left(\hat{\mathbf{R}}, \hat{\mathbf{v}}^{\text{b}}, \hat{\mathbf{B}}^{\text{b}}, \hat{\boldsymbol{\Omega}}_{\text{b}}^{\text{b/n}}, \hat{\boldsymbol{\gamma}}_{\text{b}}^{\text{b}}\right) = \hat{\mathbf{B}}^{\text{b}}$.

The filter of Eq. (8) provides an estimation of the inertial velocity smoothened by the magnetic measurement and consequently the magnetic velocity. This smoothing is conditioned by the observability of the gradient, *i.e.* the larger the gradient, the better the filtering. Moreover, the magnetic information is a strong help in the estimation of the inertial biases.

The usable output of this algorithm is the velocity of the device. Indeed, the position or relative displacement is not observable and consists, in this case, of a direct integration of the velocity through the differential equation $\dot{\hat{\mathbf{x}}}^{\text{n}} = \hat{\mathbf{R}}\hat{\mathbf{v}}^{\text{b}}$.

C. Derivation of the error model

We aim to quantify the performances of the filter designed in III-B in a comprehensive analytical formula. To do so, we design an equivalent one-dimensional toymodel filter modeling a MIDR device moving toward the curvilinear coordinate within the direction of an eigenvalue λ of the magnetic gradient. In particular, this simplification implies that the motion is nonrotative – *i.e.* there is no gyrometric data, and then no attitude[3] nor gyrometric bias to estimate. We assume two parallel single-axis magnetometers sensing data B_1 and B_2, separated by a distance $L > 0$ and symmetrically disposed at a distance $L/2$ to the center – position of the accelerometer. The gradient λ is then processed by $(B_2 - B_1)/L$ at each instant and the central field B is simply the average $(B_1 + B_2)/2$. The magnetic velocity is given by $v_{\text{mag}} = \dot{B}/\lambda$. Denote by σ_{mag}^2 the variance of the white noise of a single-axis magnetometer. The EKF (8) becomes:

$$\begin{cases} \dot{\hat{v}} & = \gamma - \hat{\gamma}_{\text{b}} \\ \dot{\hat{B}} & = \lambda\hat{v} \\ \dot{\hat{\gamma}}_{\text{b}} & = 0 \end{cases}, \quad h\left(\hat{v}, \hat{B}, \hat{\gamma}_{\text{b}}\right) = \hat{B}. \tag{9}$$

This more simple models allows to derive analytical error models. To do so, we need to state some hypotheses:

Hypothesis 1: The motion is uniform, *i.e.* the actual velocity v is constant, and *a fortiori* the acceleration γ consists in a zeros-mean white noise of variance σ_{acc}^2.

Hypothesis 2: The directional gradient λ is also constant, up to a zeros-mean white noise of variance $2\sigma_{\text{mag}}^2/L^2$. Hence, the space model of the magnetic field is linear toward the direction of λ: $B(x) = B_0 + \lambda x$, with a constant $B_0 \in \mathbb{R}$.

The errors in the estimation of the velocity can be modeled by two different sources of disturbances: static errors, *e.g.* miscalibration of the sensors; and dynamic, mainly due to noise aliasing.

The velocity error $\delta\hat{v}_{\text{noise}}$ due to noise aliasing is derived from the standard deviation of the gaussian part of $v_{\text{mag}} = \dot{B}/\lambda$:

$$\frac{\delta\hat{v}_{\text{noise}}}{v} = \frac{2\sigma_{\text{mag}}^2}{\lambda^2 L^2}, \tag{10}$$

while the error $\delta\hat{v}_{\text{calib}}$ in the estimation of the velocity due to a global static miscalibration delta δB comes from the differentiation of the kinetic equation $\dot{\hat{B}} = \lambda\hat{v}$ from Eq. (9),

$$\frac{\delta\hat{v}_{\text{calib}}}{v} = -\frac{\delta B}{\lambda L}, \tag{11}$$

for $\delta\lambda = \delta B/L$.

If the kinetic equation is completed by the knowledge of a gyrometric information – with an additional term $-\Omega B$ in the right-hand side of the kinetic equation –, then

$$\frac{\delta\hat{v}_{\text{calib}}}{v} = -\frac{\delta B}{\lambda L} + \frac{\delta\dot{B}}{\lambda v} = \frac{-\delta B/L + \delta\dot{B}/v}{\lambda}, \tag{12}$$

with $\delta\dot{B} = \Omega\delta B$ is an instationarity amplified by the miscalibration.

D. Discussion

Overall, the error of the velocity estimated from magnetic data can be represented by the following relationship

$$\frac{\text{Velocity error}}{\text{Actual velocity}} = \frac{\text{Gradient perturbation}}{\text{Actual gradient}}.$$

[2]These situations are schematic. In practice, due to the noise of the sensors, we do not have a eigenvalue perfectly equal to 0, but a small $\varepsilon > 0$ which is determined by the sensitivity of the sensors.

[3]This implies that there is no rotation between navigation and body frames, excepted a change of the origin by translation. The upperscripts n and b are hence dropped.

The depedency of this law in the gradient inverse means that the performance increases as the magnitude of the gradient grows. Therefore, what is important is the evaluation of a signal-to-noise ratio in magnetic gradient: the larger is the magnitude of the magnetic gradient, the lower the calibration errors and noise disturbs the system. Hence, in rich magnetic environments – e.g. industries, hospitals, airports, etc. – the behavior of the magnetic correction of the MIDR technology is good. However, in poor magnetic environments – *e.g.* old buildings or even for outdoor navigation – the perturbations become of the same order of magnitude as the gradient, resulting in a loss of accuracy. Moreover, the size L of the device is also important. Due to the term λL in the error law of Eq. (11), there is a direct proportionality between the magnetic gradient and the size of the device: a device twice as big, as another one, will estimate the velocity with the same accuracy in magnetic gradient twice as low.

Finally, the dimensionless parameter $v\Delta\lambda/\Delta v\lambda$, which always equals -1 due to Eq. (11), links the performance of navigation δv to the miscalibration error $\delta\lambda = \delta B/L$ and the trajectory set up (λ, v). Therefore, knowing the ratio $\delta\lambda/\lambda$, it is possible to predict the ratio $\delta v/v$ and vice versa and then to design a test trajectory set up.

IV. STEP DETECTION ALGORITHM

The velocity issued from the magnetic measurement is useful to bound the drift of an inertial navigation to an error growing only linearly in time. However, when the pedestrian moves towards a low magnetic gradient area, the magnetic velocity is too degraded. In these particular situation, the MIDR technology needs a new measurement to stabilize the velocity. Another infrastucture-free correction is used : it is an extension of the Zupt [11], [17], [18], which is too restrictive as it requires to put the navigation device at a specific location on the foot and is very sensible to shocks.

First, step detection is performed by identifying an 8 steps pattern in a typical walk motion from the inertial sensors. Then, the velocity is estimated through a walk model eliminating the part due to the leg/body relative motion [11], [15], [16].

A. Principle

The step detection with gyrometric and accelerometric data is explained in the patents [15], [16]. This technique assumes the MIDR device to be positioned at the ankle of the pedestrian.

During the "ground phase", *i.e.* when the heel is on the ground, the ankle velocity can be considered null. Consequently, the velocity is given by the cross product of the angular velocity $\boldsymbol{\Omega}^{\mathrm{b/n}}$ with the lever arm $\boldsymbol{\ell}^{\mathrm{b}}_{\mathrm{WDM}}$ between the position of the navigation point (accelerometer) and the ankle. The velocity being purely rotation-induced, its "linear" part is zero.

Definition 2: **Walk Dynamic Model (WDM).** The step detection velocity is defined as

$$\mathbf{v}^{\mathrm{b}}_{\mathrm{WDM}} = \boldsymbol{\Omega}^{\mathrm{b/n}}\boldsymbol{\ell}^{\mathrm{b}}_{\mathrm{WDM}}, \tag{13}$$

where $\boldsymbol{\ell}^{\mathrm{b}}_{\mathrm{WDM}}$ is the lever arm vector from the position of the accelerometer to the ankle of the pedestrian. Moreover, the angular velocity $\boldsymbol{\Omega}^{\mathrm{b/n}}$ is assumed to be debiased.

B. Theory

We consider now a 3D dynamic system in which the velocity $\mathbf{v}^{\mathrm{b}}$ is estimated with a velocity measurement given at each step detection. The estimation system becomes

$$\begin{cases} \dot{\hat{\mathbf{R}}} & = \hat{\mathbf{R}}\left(\boldsymbol{\Omega}^{\mathrm{b/n}} - \hat{\boldsymbol{\Omega}}^{\mathrm{b/n}}_{\mathrm{b}}\right) \\ \dot{\hat{\mathbf{v}}}^{\mathrm{b}} & = -\left(\boldsymbol{\Omega}^{\mathrm{b/n}} - \hat{\boldsymbol{\Omega}}^{\mathrm{b/n}}_{\mathrm{b}}\right)\hat{\mathbf{v}}^{\mathrm{b}} + \boldsymbol{\gamma}^{\mathrm{b}} - \hat{\boldsymbol{\gamma}}^{\mathrm{b}}_{\mathrm{b}} + \hat{\mathbf{R}}^{\top}\mathbf{g}^{\mathrm{n}} \\ \dot{\hat{\boldsymbol{\Omega}}}^{\mathrm{b/n}}_{\mathrm{b}} & = \mathbf{0} \\ \dot{\hat{\boldsymbol{\gamma}}}^{\mathrm{b}}_{\mathrm{b}} & = \mathbf{0}. \end{cases} \tag{14}$$

with a direct correction $\mathbf{y} = \mathbf{h}(\hat{\mathbf{v}}^{\mathrm{b}}) = \hat{\mathbf{v}}^{\mathrm{b}}$ thanks to an outer measurement $\mathbf{v}^{\mathrm{b}}_{\mathrm{out}}$ of the velocity.

Similarly as in section III-C and for theoretical purposes, we also analyze the equivalent one-dimensional problem

$$\begin{cases} \dot{\hat{v}} & = \gamma - \hat{\gamma}_{\mathrm{b}} \\ \dot{\hat{\gamma}}_{\mathrm{b}} & = 0 \end{cases}, \quad h(\hat{v}, \hat{\gamma}_{\mathrm{b}}) = \hat{v}, \tag{15}$$

for an outer measurement v_{out}, supposed unbiased and known with a white noise of variance $r > 0$.

However, it is very important to notice that, after convergence to its steady-state regime, the filter is still very sensitive to a static error $\delta\mathbf{v}_{\mathrm{out}}$ of $\mathbf{v}_{\mathrm{out}}$.Hence, it is crucial to choose an unbiased outer observation, otherwise the filter will converge to this static offset. This requirement is especially fulfilled by the step-detection velocity of Def. 2.

C. Correction design

We add the observation of $\mathbf{v}_{\mathrm{out}} = \mathbf{v}^{\mathrm{b}}_{\mathrm{WDM}}$ to the correction model of the EKF (8) in addition to the observation of the magnetic field. Hence, the observation becomes $\mathbf{y} = \left(\hat{\mathbf{v}}^{\mathrm{b}}_{\mathrm{WDM}}, \hat{\mathbf{B}}^{\mathrm{b}}\right)$ and the state measurement is provided by $\mathbf{h}\left(\hat{\mathbf{R}}, \hat{\mathbf{v}}^{\mathrm{b}}, \hat{\mathbf{B}}^{\mathrm{b}}, \hat{\boldsymbol{\Omega}}^{\mathrm{b/n}}_{\mathrm{b}}, \hat{\boldsymbol{\gamma}}^{\mathrm{b}}_{\mathrm{b}}\right) = \left(\hat{\mathbf{v}}^{\mathrm{b}}, \hat{\mathbf{B}}^{\mathrm{b}}\right)$.

The global designed MIDR-EKF with WDM correction is presented on Fig. 2.

D. Expected behaviors and results

The WDM works as an additional velocity sensor (on top of magnetic velocity), with a much lower frequency but also a more consistent - and often better - accuracy, since it does not depend on the magnetic environment.

Therefore, it is most useful in low-gradient areas, preventing the filter from diverging when magnetic measurements are not reliable enough.

In more favorable magnetic environments, it also leads to better convergence.

In terms of filter states, since it has the same observation matrix as the magnetic velocity – identity along velocity –, given sufficient time it also enables the convergence of the IMU biases states and consequently the estimated attitude.

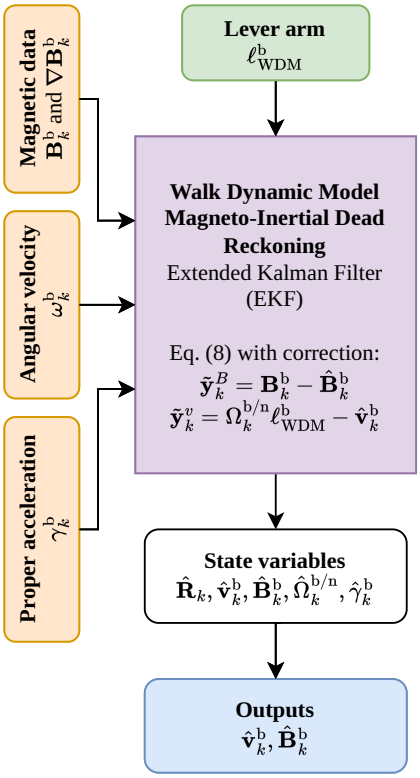

Fig. 2: Global MIDR-EKF with velocity correction through walk dynamic model. The dynamic inputs – *i.e.* sensors data – are provided in orange, whereas constant input – the lever arm – is in green. The algorithmical block is in purple, wrapping the correction term in magnetic field and in velocity. The outputs, in blue, consist in the velocity and the magnetic field only.

V. FUSION OF CORRECTION METHODS

A. Experiments

This section presents the results of a series of experi- ments comparing the performance of the classic MIDR algorithms with the improved version proposed here relying on a velocity derived from a walk motion model at each step detected.

Both use exactly the same set of sensors, *i.e.* accelerometers, gyrometers and magnetometers. In order to obtain the trajectories from both algorithms, we first recorded the measurements in real time, before replaying them with each algorithm separately.

The studied trajectory starts with a specifically designed challenging outdoor phase with low magnetic gradient to assess classical MIDR navigation in the worst case. Starting from a car park, the user walks 100 m on the sideway until he reaches the entrance of a building. The user then proceeds to walk for a few minutes inside the building, on three different levels.

Several precisely geolocalized tags are present inside and oustide the building[4]; a trajectory consists in a series of segment between two of these tags. Each time the person wearing the navigation system reaches one of them, the timetag is saved, enabling a precise *a posteriori* evaluation of the position error from our navigation system.

The MDIR navigation being relative (no absolute position observation), the first tag serves as the trajectory initialization point. While the measurement of the magnetic North gives a good approximation of the trajectory absolute orientation, here the initial heading is also provided so that the ground trace can be adjusted to the building map.

Since the trajectory is a series of segments between known points, the performance evaluation measurements used to track the navigation performance will revolve around per-segment position errors, both absolute and relative to the walked distance. In order to track the accuracy on longer periods and provide a global evaluation of the navigation performance, the cumulated error will also be evaluated.

Finally, the indoor/outdoor distinction is not important in terms of "physical" environment, but it rather marks an important change of magnetic environment. Thus, as the test building contains numerous metallic parts, the magnetic gradient is quite high inside, while it tends to be very low outside.

Therefore, the subsequent analysis can be interpreted in terms of favourable/unfavourable magnetic environment rather than indoor/outdoor navigation.

B. Qualitative trajectories analyses

Fig. 3 compares the trajectories obtained with the MIDR navigation and the step-detection aided WDM-MIDR. As expected, both look very similar inside the building, which is recent and full of metallic materials, providing a favorable magnetic environment: the magnetic velocity by itself is therefore already of high quality[5] However, one can clearly see that, outside the building, the classic MIDR navigation struggles to keep a consistent course, alternating between stable and unstable phases in the intentionally challenging environment chosen for the experiments. On the other hand, the step-detection keeps the navigation point on track, and seems to accurately follow the sidewalk, not intersecting the building on its way. The main objective of the step-detection aided MIDR algorithm is hence to improve the travelled distance estimation. In itself, the heading remains similar to the classic MIDR algorithm.

C. Quantitative trajectories analyses

Fig. 4 shows the segment by segment error and cumulated errors. Apart from the first segment, ranging from the parking (common initialization tag) to the building north side for an approximate 80m length, each segment has a length of around 5 to 20 m. The performance gain between step-detection aided

[4]The positions of these tags have been accurately determined by topographical methods.

[5]The zoomed trajectories were adjusted to the building map, such that it is possible to see the relative accuracy for the indoor phase, independently from the outdoor navigation drift.

Fig. 3: Outdoor + Indoor trajectory using classic magneto-inertial (blue) and step-detection aided (red) navigation. Above: full trajectory, below: zoom on building plan (with cancelled outdoor drift).

and nonaided navigations is significant during the first three segments, which correspond to the outdoor phase, for which the magnetic gradient was purposely chosen to be low. The improvement is in particular noticeable for segment #2, which was specifically designed to be a worst case scenario for classic MIDR navigation. Indeed, MIDR yields an error of about 6 m while a WDM aided one dramatically reduces the error to about 0.5 m in this particular instance.

Several indoor/outdoor trajectories, comparable in size to the one presented above (from 200 m to 300 m), were

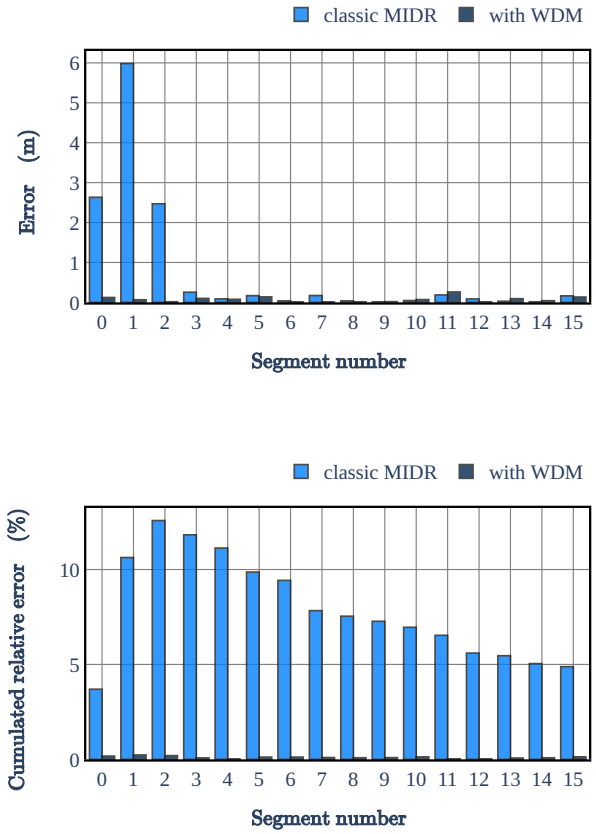

Fig. 4: 3D error norm per trajectory segment (up), and cumulated error divided by total distance (down)

performed with 4 different MIMU devices on various magnetic environments. The outdoor parts last about 100 s and the indoor sections roughly 150 s.

Table I presents the performance of both algorithms (with and without Walk Dynamic Model – WDM), averaged on 2 categories of magnetic environments (12 runs each): both categories contain trajectories with indoor/outdoor segments. The "low gradient" category contains trajectories with a specific outdoor phase along very low magnetic areas, materializing a worst case scenario for MDIR navigation. However, it is not representative of a nominal *indoor* pedestrian trajectory.

These results again point out that the WDM-MIDR algorithm significantly improves the results for low average magnetic gradient (panel #1) by a factor 7. The results of panel #2 are naturally better due to higher gradients, and the WDM-MIDR maintain the navigation accuracy.

D. Discussion

In a "model-based" measurement such as the WDM we are using here, the main limitation usually comes from the accuracy of the model itself. Thus, while the ankle-navigation movement was considered to be purely angular, this was not exactly correct as the foot never reaches a perfectly zero-

TABLE I: Cumulated 3D error norm as a percentage of the total walked distance, for the classic MIDR and Walk Dynamic Model MIDR (WDM-MIDR) algorithms.

Panel	**MIDR**	**WDM-MIDR**	**Average gradient** (G/m)
Low gradient[6]	6.9%	0.9%	0.02
High gradient	0.7%	0.7%	0.13

velocity stationary state on the ground. This inaccuracy is especially emphasized if the person walks very quickly – *i.e.* with the heel "bouncing" on the ground –, or worse, runs. The second source of error comes from the knowledge of the terms $\boldsymbol{\Omega}^{\mathrm{b/n}}\boldsymbol{\ell}^{\mathrm{b}}_{\mathrm{WDM}}$ and particularly the identification and measurement of the lever arm $\boldsymbol{\ell}^{\mathrm{b}}_{\mathrm{WDM}}$. While the angular velocity is relatively well-known thanks to the gyrometers, the lever arm is roughly estimated with standard values, leading to a constant error on the velocity "measurement".

These imperfections do not prevent us from reaching a 1% accuracy in position, but a more complex walk model or a better knowledge of the lever arm would allow for even more precise navigation.

VI. CONCLUSIONS

This article proposed a major improvement of magneto-inertial dead reckoning navigation. It defined a new velocity update step of the MIDR Kalman filter based on the detection of walking steps and dynamical modelling of the walk itself (WDM). The new fusion algorithm was implemented and experimented with real magneto-inertial devices on outdoor/indoor trajectories. The results showed that the new step-detection aided MIDR algorithm yields a reduction by a factor about 7 of the travelled distance estimation error in poor magnetic environments.

Outdoor navigation is generally the first step to initialize indoor navigation, and the addition of a walk model to the MIDR will improve the transitions between indoor and outdoor phases. The WDM aided navigation is thus a significant stepforward for resilient pedestrian navigation in diverse environments.

REFERENCES

[1] B.D.O. Anderson, J.B. Moore. *Optimal Filtering*, Dover Publications, Inc., Mineola, New York, 357 pages, 1979.

[2] C.-I. Chesneau, M. Hillion, and C. Prieur, "Motion estimation of a rigid body with an EKF using magneto-inertial measurements," in *2016 International Conference on Indoor Positioning and Indoor Navigation* (IPIN), (Alcalá de Henares, Spain), oct 2016.

[3] C.-I. Chesneau, M. Hillion, J.-F. Hullo, G. Thibault, and C. Prieur, "Improving magneto-inertial attitude and position estimation by means of a magnetic heading observer," in *2017 International Conference on Indoor Positioning and Indoor Navigation* (IPIN), (Sapporo, Japan), sep 2017.

[4] C.-I. Chesneau, R. Robin, H. Meier, M. Hillion, C. Prieur. "Calibration of a magnetometer array using motion capture equipment," Asian Journal of Control, Asian Control Association (ACA) and Chinese Automatic Control Society (CACS) 2019, 21 (4), pp.1459-1469. 10.1002/asjc.2043. hal-02368023.

[5] C.-I. Chesneau. *Magneto-Inertial Dead-Reckoning in inhomogeneous field and indoor applications*, Doctoral dissertation, Université Grenoble Alpes, 2018.

[6] C. Huang, G. Hendeby, I. Skog, "A Tightly-Integrated Magnetic-Field aided Inertial Navigation System", 8 pages, 2022.

[7] R. Neymann, H. Meier, H. Lhachemi, C. Prieur, A. Girard. "Minimization of Parameter Sensitivity to Pre-Estimation Errors and its Application to the Calibration of Magnetometer Arrays," 2023.

[8] N. Praly, N. Petit, J. Laurent-Varin, "Using distributed magnetometry in navigation of heavy launchers and space vehicles," 4th European Conference for Aerospace Sciences (EUCASS), Jul 2011, St Petersburg, Russia. hal-00617906.

[9] V. Renaudin, M. Haris Afzal, G. Lachapelle. "Complete Triaxis Magnetometer Calibration in the Magnetic Domain," Hindawi Publishing Corporation, *Journal of Sensors*, Volume 2010, Article ID 967245, 10 pages. doi:10.1155/2010/967245.

[10] P. G. Savage. *Strapdown Analytics*. Strapdown Associates, 2000.

[11] I. Skog, P. Händel, J.-O. Nilsson. "Zero-Velocity Detection—An Algorithm Evaluation," in *IEEE Transactions on Biomedical Engineering*, vol. 57, no. 11, pp 2657-2666, nov 2010.

[12] I. Skog, G. Hendeby, and F. Gustafsson, "Magnetic odometry - a model-based approach using a sensor array," in *International Conference on Information Fusion* (FUSION), Cambridge, United Kingdom, pp. 794–798, 2018.

[13] D. Vissière, A. Martin, and N. Petit, "Using distributed magnetometers to increase imu-based velocity estimation into perturbed area," in Conference on Decision and Control (CDC), (New Orleans, LA), pp. 4924–4931, 2007.

[14] D. Vissière, A. Martin, and N. Petit, "Système fournissant la vitesse et la position d'un corps en utilisant les variations du champ magnétique évaluées grâce aux mesures de un ou des magnétomètres et de une ou des centrales inertielles," Patent FR2914739 (A1), 2008.

[15] D. Vissière, M. Hillion, E. Dorveaux, A. Jouy, M. Grelet, Brevet PCT/FR2016/052619, "Procédé d'estimation du mouvement d'un piéton", 2016.

[16] D. Vissière, M. Grelet, Brevet PCT/FR2019/243609, "Analyse de la foulée d'un piéton en marche", 2019.

[17] M. Zmitri, H. Fourati, C. Prieur. "Magnetic Field Gradient-Based EKF for Velocity Estimation in Indoor Navigation," in *Sensors*, no. 20, p. 5726, 2021.doi: 10.3390/s20205726.

[18] M. Zmitri, H. Fourati and C. Prieur, "BiLSTM Network-Based Extended Kalman Filter for Magnetic Field Gradient Aided Indoor Navigation," in IEEE *Sensors Journal*, vol. 22, no. 6, pp. 4781-4789, 2022, doi: 10.1109/JSEN.2021.3091862.